Published in final edited form as:
Gastroenterology. 2009 April ; 136(4): 1368–1378. doi:10.1053/j.gastro.2008.12.066.

Loss of the Acinar-Restricted Transcription Factor Mist1 Accelerates Kras-Induced Pancreatic Intraepithelial Neoplasia

Guanglu Shi[*,1], **Liqin Zhu**[*,1], **Yan Sun**[1], **Ryan Bettencourt**[1], **Barbara Damsz**[1], **Ralph H. Hruban**[2], and **Stephen F. Konieczny**[1]

[1]Department of Biological Sciences and the Purdue Cancer Center, Purdue University, West Lafayette, IN

[2]Departments of Pathology and Oncology, Sol Goldman Pancreatic Cancer Research Center, Johns Hopkins University School of Medicine, Baltimore, MD

Abstract

Background & Aims—Invasive pancreatic ductal adenocarcinoma is thought to originate from duct-like lesions called pancreatic intraepithelial neoplasia (PanIN). PanINs progress from low grade (PanIN-1) to high grade (PanIN-3) as the cells attain molecular alterations to key regulatory genes, including activating mutations in the *KRAS* protooncogene. Despite a well documented progression model, our knowledge of the initiator cells of PanINs and the transcriptional networks and signaling pathways that impact PanIN formation remains incomplete.

Methods—In this study, we examined the importance of the acinar-restricted transcription factor Mist1 to $Kras^{G12D}$-induced mouse PanIN (mPanIN) formation in three different mouse models of pancreatic cancer.

Results—In the absence of Mist1 ($Mist1^{KO}$), $Kras^{G12D}$ expressing mice exhibited severe exocrine pancreatic defects that were rescued by ectopic expression of Mist1 in acinar cells. Mouse PanIN development was greatly accelerated in $Mist1^{KO}/Kras^{G12D/+}$ pancreata and *in vitro* assays revealed that $Mist1^{KO}$ acinar cells were predisposed to convert to a ductal phenotype and activate EGFR and Notch signaling pathways.

Conclusions—We propose that convergence of EGFR, Notch and Kras pathways in acinar cells lacking Mist1 leads to enhanced mPanIN formation.

Introduction

With a five-year survival rate of less than 5%, pancreatic ductal adenocarcinoma (PDA) is among the most lethal of all human malignancies [1, 2]. The factors responsible for this frightening statistic include the resistance of pancreatic cancers to conventional chemotherapy and radiotherapy and the absence of early warning signs and symptoms. Despite a number of

Corresponding Author: Stephen F. Konieczny, Department of Biological Sciences and the Purdue Cancer Center, Purdue University, Hansen Life Sciences Research Building, 201 South University Street, West Lafayette, IN 47907-2064, Tel: 765-494-7976, sfk@purdue.edu.
*these authors contributed equally to this work.

No conflicts of interest exist

advances in basic and clinical pancreas biology, our understanding of the pathogenesis and the molecular mechanisms underlying PDA remain incomplete.

Three different ductal precursor lesions have been identified which give rise to invasive PDA - pancreatic intraepithelial neoplasia (PanIN), intraductal papillary mucinous neoplasia (IPMN), and mucinous cystic neoplasia (MCN) [3-5]. Of these, PanINs are the best characterized, being classified from low grade (PanIN-1) to high grade (PanIN-3) based on a number of histological criteria including the degree of architectural and nuclear atypia. Activating mutations in the *KRAS2* protooncogene are thought to be the initiating mutations responsible for PanIN-1 lesions [4]. Additional genetic modifications include telomere shortening, inactivation of the $p16^{INK4a}$ locus (PanIN-2), and inactivation of the *TP53*, *SMAD4/DPC4* genes (PanIN-3) [6-9]. Alterations in these oncogenes and tumor suppressor genes cause pleiotropic effects that lead to the deregulation of signaling pathways controlling cell proliferation, survival, adhesion and migration [2, 10].

In an effort to model PDA, a number of mutant mouse strains have been developed that overexpress an activated *Kras* oncogene within specific pancreatic cellular compartments [11-14] or that conditionally activate a mutant *Kras* allele from it's own endogenous locus [15-18]. In many instances, $Kras^{G12D}$ expressing mice develop PanINs (referred to as mPanINs in mice) that on rare occasions progress to PDA after a long latency period (>1 year). While PanINs can be modeled in mice, the identity of the initial target cell remains controversial. Although the histological features of PanINs suggest a duct cell origin, several studies have proposed that acinar cells also may participate in PanIN development [10, 14, 17, 19-21].

The successful establishment of mouse models that mimic human disease has been a significant breakthrough in pancreatic oncology, although the role of individual transcription networks in PanIN development has not been fully studied. As a first step, we examined the importance of Mist1, a basic helix-loop-helix transcription factor that is expressed in pancreatic acinar cells but not in duct, islet, or centroacinar cells [20, 22, 23]. To investigate the importance of Mist1 and acinar cells to mPanIN initiation, we focused on the early events of mPanIN development in three different mutant $Kras^{G12D}$ model systems - $Mist1^{Kras/+}$ mice in which a $Kras^{G12D}$ coding region was targeted to the *Mist1* locus [13], *LSL-*$Kras^{G12D/+}$/$ptf1a^{Cre/+}$ mice in which an endogenous $Kras^{G12D}$ allele was expressed upon "pan" pancreas Cre expression [16, 24], and *LSL-*$Kras^{G12D/+}$/$Mist1^{Cre-ER/+}$ mice in which the endogenous $Kras^{G12D}$ allele was expressed in adult acinar cells upon tamoxifen addition. Our studies revealed that in the absence of Mist1, $Mist1^{Kras/LacZ}$ mice exhibited gross pancreatic defects that could be rescued by ectopic expression of Mist1 in acinar cells. Similarly, mPanIN formation in *LSL-*$Kras^{G12D/+}$/$ptf1a^{Cre/+}$ and *LSL-*$Kras^{G12D/+}$/$Mist1^{Cre-ER/+}$ mice was greatly accelerated in the absence of Mist1, suggesting that *Mist1* null acinar cells either locally influenced duct cells or directly converted to mPanINs. Indeed, lineage tracing studies confirmed that mPanINs from *LSL-*$Kras^{G12D/+}$/$Mist1^{Cre-ER/Cre-ER}$ mice were derived from adult acinar cells. Interestingly, *in vitro* assays demonstrated that $Mist1^{LacZ/LacZ}$ cells were predisposed to convert to a ductal phenotype and activate key EGFR and Notch signaling pathways that cooperated with $Kras^{G12D}$. We conclude that loss of Mist1 leads to enhanced $Kras^{G12D}$-induced mPanIN formation in these mouse models.

Materials and Methods

Mouse strains

$Mist1^{KrasG12D/+}$ ($Mist1^{Kras/+}$) mice [13] were crossed to $Mist1^{LacZ/LacZ}$ mice [25] to generate $Mist1^{Kras/LacZ}$ mice. The $elastase_{pr}$-$Mist1^{myc}$ (El_{pr}-$Mist1^{myc}$) construct driving acinar-specific expression of a myc-tagged Mist1 protein was used to produce El_{pr}-$Mist1^{myc}$ transgenic mice as described previously [26]. $Mist1^{Cre-ER/+}$ mice were generated by standard ES cell targeting in

which the complete *Mist1* coding region was replaced with the Cre-ER^{T2} coding region [27]. *LSL-Kras*$^{G12D/+}$ and *ptf1a*$^{Cre/+}$ strains were crossed to *Mist1*$^{LacZ/LacZ}$ mice to generate *Mist1*$^{LacZ/LacZ}$/*LSL-Kras*$^{G12D/+}$/*ptf1a*$^{Cre/+}$ mice. Similarly, *LSL-Kras*$^{G12D/+}$/*Mist1*$^{Cre-ER/Cre-ER}$ mice were generated by standard crosses. Induction of Cre-ER^{T2} activity was accomplished by providing adult mice (>6 weeks) tamoxifen (4 mg/mouse/day) for 3 consecutive days. All studies were conducted in compliance with NIH and the Purdue University IACUC guidelines.

Histology and immunohistochemistry

Mouse pancreas tissues were processed as previously described [20]. Primary antibodies included rabbit amylase (Calbiochem, San Diego, CA), mouse β-gal, mouse myc (9E10), and rat K19 (TROMA-3) (Developmental Studies Hybridoma Bank, Iowa City, IA), rabbit Hes1 (gift of Tetsuo Sudo), mouse Ki67 (Novocastra, Newcastle Upon Tyne, UK), mouse phospho-Stat3 (Upstate, Lake Placid, NY), rabbit insulin (Linco Research, St. Louis, MO), and rabbit Mist1 [22, 25].

Protein immunoblot assays

20 μg of whole cell protein extracts were separated on 12% acrylamide gels, transferred to PVDF membranes and incubated with primary antibodies (1:1000) against rabbit Mist1 [22, 25], mouse myc (9E10, Developmental Hybridoma Bank), rabbit ErbB1, rabbit phospho-MEK1/2 (Ser217/221), rabbit phospho-ERK (Thr202/204), rabbit phospho-Akt (Ser473) (Cell Signaling, Danvers, MA), and mouse phospho-Stat3 (Upstate, Lake Placid, NY). Detection of Hsp90 with rabbit Hsp 90a/b (1:2000, Santa Cruz, Santa Cruz, CA) was used as a loading control. Immunoblots were developed using an ECL kit (Pierce, Rockford, IL) as per manufacturer's instructions.

RNA expression analysis

Pancreas RNA was isolated using the RNeasy isolation system (QIAGEN, Valencia, CA) and reverse transcribed using the iScript™ cDNA synthesis kit (Bio-Rad, Hercules, CA). PCR conditions are described in Supplemental Data.

Acinar cell cultures

Primary acinar cells were isolated from wild type or *Mist1*$^{LacZ/LacZ}$ mice as described by Means et al. [28]. After plating in 1.35 mg/ml collagen (BD biosciences, San Jose, CA), the cells were supported with RPMI medium (Invitrogen, Carlsbad, CA) supplemented with 1% FBS, 0.1 mg/ml soybean trypsin inhibitor, 1 μg/ml dexamethasone, 100 units/ml penicillin and 100 μg/ml streptomycin. TGFα (10 ng/ml or 50 ng/ml) (R&D systems, Minneapolis, MN) was added to the medium and the efficiency of acinar-to-ductal conversion was measured after 5 days.

Results

Mist1 is essential for survival of Mist1$^{Kras/+}$ mice

Previous studies showed that pancreata from *Mist1*$^{Kras/+}$ mice had significantly lower levels of the acinar-restricted transcription factor Mist1 [13]. In order to establish if loss of Mist1 protein was critical to the *Mist1*$^{Kras/+}$ phenotype, we generated *Mist1*$^{Kras/LacZ}$ animals that expressed Kras^{G12D} and β-gal from the *Mist1* locus but lacked Mist1 protein. Although *Mist1*$^{Kras/LacZ}$ mice appeared normal at birth, they rapidly lost body weight, became dehydrated, and died within three days (Figure 1A). Newborn animals had a significantly enlarged pancreas that was ~10-fold larger than *Mist1*$^{LacZ/+}$ mice and ~2.5-fold larger than *Mist1*$^{Kras/+}$ mice (Figure 1B). As expected, control newborn *Mist1*$^{LacZ/+}$ animals exhibited normal acini and islet organization (Figure 1C, a). *Mist1*$^{Kras/+}$ pancreata also retained relatively normal exocrine

organization with the exception that the lumina of the acini were often dilated, revealing early signs of acinar metaplasia (Figure 1C, b) [13]. In older animals (2-3 months), the presence of acinar/duct biphenotypic cells was readily observed as acinar cells transitioned to a duct-like cell (Supplemental Figure S1) [13, 20]. In contrast to *Mist1*$^{Kras/+}$ mice, *Mist1*$^{Kras/LacZ}$ pancreata were grossly distorted at birth, consisting of extensive epithelial tubular networks in which the normal apical-basal polarity of secretory granules, nuclei, and endoplasmic reticulum was lost and individual cell boundaries were difficult to distinguish (Figure 1C, c-f). The zymogen-containing tubular cells also co-expressed keratin 19 (K19) (Supplemental Figure S1), suggesting a greatly accelerated acinar-ductal conversion for *Mist1*$^{Kras/LacZ}$ acinar cells. Despite the dramatic exocrine pancreas phenotype, insulin-positive islets appeared normal in *Mist1*$^{Kras/LacZ}$ animals (Supplemental Figure S2).

The highly disrupted organization of *Mist1*$^{Kras/LacZ}$ pancreata prompted us to investigate if alterations in cellular proliferation were associated with constitutive Kras signaling in the absence of Mist1. Analysis of newborn *Mist1*$^{+/+}$ or *Mist1*$^{LacZ/+}$ pancreata revealed a substantial number of Ki67 positive cells, but the vast majority were either duct cells or stellate cells that were located within the interstitial spaces surrounding acinar structures (Figure 1C, g). Very few (6%) proliferating acinar cells were detected at this age. In contrast, 35% of *Mist1*$^{Kras/+}$ acinar cells were Ki67 positive (Figure 1C, h). Interestingly, *Mist1*$^{Kras/LacZ}$ pancreata exhibited an even greater increase in cell proliferation where >80% of the cells expressed Ki67 (Figure 1C, i). TUNEL assays failed to reveal any significant apoptotic activity (data not shown), suggesting that the extensive proliferation of *Mist1*$^{Kras/LacZ}$ cells likely accounts for the dramatic expansion of the duct-like lesions in this model.

Finally, to determine if ectopic Mist1 expression from a different acinar-specific promoter could rescue *Mist1*$^{Kras/LacZ}$ mice, we crossed *Mist1*$^{Kras/+}$ mice to *Mist1*$^{LacZ/LacZ}$ mice containing an *elastase* promoter-Mist1^{myc} transgene (*El*$_{pr}$*-Mist1*^{myc}) (Figure 2A). As predicted, Mist1^{myc} protein was detected only in acinar cells in *Mist1*$^{LacZ/LacZ}$/*El*$_{pr}$*-Mist1*^{myc} samples (Figure 2B, a-b). Islet and duct cells remained Mist1^{myc} negative. Similarly, *Mist1*$^{Kras/LacZ}$ pancreata were Mist1 negative whereas the *El*$_{pr}$*-Mist1*^{myc} transgene was expressed in *Mist1*$^{Kras/LacZ}$/*El*$_{pr}$*-Mist1*^{myc} acinar cells (Figure 2C, a). Unlike the severe phenotype of *Mist1*$^{Kras/LacZ}$ pancreata, *Mist1*$^{Kras/LacZ}$/*El*$_{pr}$*-Mist1*^{myc} pancreata displayed a phenotype that was virtually identical to *Mist1*$^{Kras/+}$ mice (Figure 2C, b-c). *Mist1*$^{Kras/LacZ}$/*El*$_{pr}$*-Mist1*^{myc} mice survived for months and acinar organization was largely restored, although areas of acinar metaplasia were similarly observed as in *Mist1*$^{Kras/+}$ animals. As predicted, the number of Ki67-positive cells also was significantly reduced (~40%) in *Mist1*$^{Kras/LacZ}$/*El*$_{pr}$*-Mist1*^{myc} mice. These results confirm that the absence of Mist1 promotes Kras^{G12D}-induced cell proliferation and dramatically enhances pancreas transformation.

Loss of Mist1 accelerates mPanIN initiation in LSL-Kras$^{G12D/+}$/ptf1a$^{Cre/+}$ mice

Mist1$^{Kras/+}$ mice undergo acinar-ductal metaplasia and develop invasive and metastatic pancreatic cancer [13], but in the absence of Mist1 protein the mice die shortly after birth, preventing a detailed analysis of early precursor lesions. To examine the importance of Mist1 to mPanIN initiation events, we turned to the Cre-activated *LoxP-STOP-LoxP(LSL)-Kras*$^{G12D/+}$ model which produces mPanINs when pancreas-restricted *Cre* expression is provided by *pdx1*$_{pr}$*-Cre* or *ptf1a*$^{Cre/+}$ mouse lines [16, 20]. *Mist1*$^{LacZ/LacZ}$/*LSL-Kras*$^{G12D/+}$/*ptf1a*$^{Cre/+}$ mice were generated by crossing *LSL-Kras*$^{G12D/+}$/*ptf1a*$^{Cre/+}$ mice to *Mist1*$^{LacZ/LacZ}$ mice. At 6 weeks of age, control *LSL-Kras*$^{G12D/+}$/*ptf1a*$^{+/+}$ mice (lacking Cre) exhibited average sized pancreata with normal histological features (Figure 3A). As previously reported [16], *Mist1*$^{+/+}$/*LSL-Kras*$^{G12D/+}$/*ptf1a*$^{Cre/+}$ mice developed slightly enlarged pancreata that otherwise had normal gross structure. In contrast, *Mist1*$^{LacZ/LacZ}$/*LSL-Kras*$^{G12D/+}$/

ptf1a$^{Cre/+}$ pancreata were significantly larger than pancreata from control littermates, paralleling the increased size phenotype of *Mist1*$^{Kras/LacZ}$ mice (Figure 3A).

We next compared mPanIN initiation and progression between *LSL-Kras*$^{G12D/+}$/*ptf1a*$^{Cre/+}$ mice maintained on a *Mist1*$^{+/+}$ or *Mist1*$^{LacZ/LacZ}$ genetic background. Animals of both genotypes showed rare mPanIN-1A lesions surrounded by normal acinar structures at 3 weeks of age (data not shown). However, mPanIN lesions developed much more rapidly in *Mist1*$^{LacZ/LacZ}$/*LSL-Kras*$^{G12D/+}$/*ptf1a*$^{Cre/+}$ mice where mPanIN-1A lesions were commonly seen at 4 weeks and by 6 weeks mPanIN-1A distribution was extensive throughout the entire pancreas (Figure 3B,C, b-e). Contrary to these results, mPanIN formation in 6 week *Mist1*$^{+/+}$/*LSL-Kras*$^{G12D/+}$/*ptf1a*$^{Cre/+}$ animals remained rare and focally localized (Figure 3C, a). Significantly, high grade mPanIN-2 and mPanIN-3 lesions were also much more abundant in *Mist1*$^{LacZ/LacZ}$/*LSL-Kras*$^{G12D/+}$/*ptf1a*$^{Cre/+}$ mice (Figure 3B,C, c-e). As predicted, *Mist1*$^{LacZ/LacZ}$/*LSL-Kras*$^{G12D/+}$/*ptf1a*$^{Cre/+}$ mPanINs displayed features common to human PanINs, including elevated levels of mucin, expression of the duct-restricted marker K19, and activation of Notch downstream signaling targets such as Hes1 (Figure 3C, f-h). Cells within *Mist1*$^{LacZ/LacZ}$/*LSL-Kras*$^{G12D/+}$/*ptf1a*$^{Cre/+}$ mPanINs were also highly proliferative (Figure 3C, i). Interestingly, real-time RT-PCR revealed a dramatic change from acinar gene products (amylase) to duct gene products (K19) in 6 week *Mist1*$^{LacZ/LacZ}$/*LSL-Kras*$^{G12D/+}$/*ptf1a*$^{Cre/+}$ pancreata (Supplemental Figure S3), suggesting a switch from predominantly acinar to predominantly ductal cell types in young mice expressing *Kras*^{G12D} but lacking Mist1. Whether this reflects a conversion of acinar cells to ductal cells is not known, but acinar cells clearly contribute to mPanIN formation in this model since β-gal positive cells (expressed from the *Mist1* locus) were readily observed in mPanINs of *Mist1*$^{LacZ/LacZ}$/*LSL-Kras*$^{G12D/+}$/*ptf1a*$^{Cre/+}$ pancreata (Figure 3C, j-l) [20].

LSL-Kras$^{G12D/+}$/Mist1$^{Cre-ER/Cre-ER}$ mice reveal that Mist1 null acinar cells readily generate advanced mPanINs upon Kras^{G12D} expression

The presence of β-gal+ cells in mPanINs from *Mist1*$^{LacZ/+}$/*LSL-Kras*$^{G12D/+}$/*ptf1a*$^{Cre/+}$ and *Mist1*$^{LacZ/LacZ}$/*LSL-Kras*$^{G12D/+}$/*ptf1a*$^{Cre/+}$ mice suggested that *Kras*^{G12D} expressing acinar cells are the major cellular source of mPanINs in this model. In order to examine this in greater detail, we generated *Mist1*$^{Cre-ER/+}$ mice in which the complete *Mist1* coding region was replaced with a Cre-ER^{T2} coding region. Using the R26R reporter line, tamoxifen-induced Cre activity was observed primarily in *Mist1*$^{Cre-ER/+}$ acinar cells although a small percentage (<3%) of islet cells also exhibited β-gal activity (Figure 4A, a-b). Importantly, all cells from small and large ducts remained β-gal negative, confirming that the *Mist1* locus is not expressed in this pancreas compartment. Administering tamoxifen to 6 week *LSL-Kras*$^{G12D/+}$/*Mist1*$^{Cre-ER/+}$ mice lead to mPanIN-1A formation that mimicked the pattern observed with *LSL-Kras*$^{G12D/+}$/*ptf1a*$^{Cre/+}$ mice (Figure 4B, a-c). Similarly, tamoxifen induction in adult *LSL-Kras*$^{G12D/+}$/*Mist1*$^{Cre-ER/Cre-ER}$ mice (lacking Mist1) also readily generated mPanINs, but in this instance the number and grade of mPanINs was greatly accelerated, paralleling the results obtained with *Mist1*$^{LacZ/LacZ}$/*LSL-Kras*$^{G12D/+}$/*ptf1a*$^{Cre/+}$ mice. mPanIN-2 and mPanIN-3 lesions with atypical nuclei and large papillary extensions were often observed fusing to normal ductal epithelial (Figure 4B, d-f, 4C). As predicted, the mPanINs from *LSL-Kras*$^{G12D/+}$/*Mist1*$^{Cre-ER/Cre-ER}$ mice exhibited duct cell characteristics, including expression of K19 (Figure 4B, g). R26R lineage tracing of *LSL-Kras*$^{G12D/+}$/*Mist1*$^{Cre-ER/Cre-ER}$ mice confirmed the acinar cell origin of the advanced mPanINs in which virtually all expressed β-gal whereas duct cells remained β-gal negative (Figure 4B, h). Based on these results, we conclude that the absence of Mist1 promotes *Kras*^{G12D}-expressing acinar cells to form ductal mPanINs.

EGFR signaling is hyperactive in Kras^{G12D} expressing cells lacking Mist1

Several studies have shown that EGFR signaling can induce acinar cells to transition to duct-like cells in a number of pancreatic cancer mouse models [20, 21, 29, 30]. The increased propensity by which loss of Mist1 and Kras signaling generates mPanIN lesions also suggests that *Mist1*$^{LacZ/LacZ}$ cells are primed to influence mPanIN formation, possibly through activation of EGFR downstream signaling pathways. To evaluate if EGFR signaling components are differentially active in *Mist1*$^{LacZ/LacZ}$ and *LSL-Kras*$^{G12D/+}$/*ptf1a*$^{Cre/+}$ animals, 6 week pancreata from different mouse genotypes were isolated and processed for real-time RT-PCR, immunoblot, and immunohistochemistry analyses. As shown in Figure 5A, transcript levels for the EGFR family members *ErbB1* and *ErbB2*, as well as the target ligands *TGFα* and *HB-EGF*, were not significantly different between control *Mist1*$^{+/+}$/*LSL-Kras*$^{G12D/+}$ (WT) and *Mist1*$^{+/+}$/*LSL-Kras*$^{G12D/+}$/*ptf1a*$^{Cre/+}$ (WT + Kras) animals. In contrast, moderate (2-3-fold) increases in *ErbB1* and *TGFα* transcript levels were always observed in *Mist1*$^{LacZ/LacZ}$/*LSL-Kras*$^{G12D/+}$ (KO) animals (Figure 5A). However, when the *Mist1*$^{LacZ/LacZ}$ genotype was combined with active Kras^{G12D} (KO + Kras) large (30-500-fold) increases in *ErbB1*, *ErbB2*, *TGFα*, and *HB-EGF* transcripts were produced (Figure 5A).

Immunoblot analyses on additional animals confirmed that the levels of ErbB1 were increased in the *Mist1*$^{LacZ/LacZ}$/*LSL-Kras*$^{G12D/+}$/*ptf1a*$^{Cre/+}$ pancreata (Figure 5B). As predicted, components of the MAPK pathway were also activated, including elevated levels of phospho-MEK1/2 and phospho-Erk1/2 (Figure 5B). Interestingly, these pathways were similarly active in control *Mist1*$^{LacZ/LacZ}$/*LSL-Kras*$^{G12D/+}$ samples lacking Mist1 and Kras^{G12D} protein (KO). Stat3, another downstream effector of the ErbB pathway [31], was also activated in the *Mist1*$^{LacZ/LacZ}$ samples. Indeed, immunohistochemistry confirmed that the increase in pStat3 levels was exclusively due to expression in acinar cells (Figure 5C). These results reveal that loss of Mist1 triggers MAPK and Stat3 signaling in acinar cells and suggest that the extreme phenotype associated with *Mist1*$^{LacZ/LacZ}$/*LSL-Kras*$^{G12D/+}$/*ptf1a*$^{Cre/+}$ and *LSL-Kras*$^{G12D/+}$/*Mist1*$^{Cre-ER/Cre-ER}$ animals is due to a convergence of signaling components involving Kras^{G12D} expression and hyperactivity of the EGFR pathway in the absence of Mist1.

Mist1$^{LacZ/LacZ}$ acinar cells rapidly convert to duct-like cells in 3D cultures

The large increase in mPanINs in very young *Mist1*$^{LacZ/LacZ}$/*LSL-Kras*$^{G12D/+}$/*ptf1a*$^{Cre/+}$ and *LSL-Kras*$^{G12D/+}$/*Mist1*$^{Cre-ER/Cre-ER}$ animals suggested that *Mist1*^{KO} pancreata are highly sensitive to Kras^{G12D} signaling events and that the response to *Kras*^{G12D} expression may induce acinar cells to develop duct-like properties, including expression of K19, formation of tubular complexes, and participation in mPanIN formation. Indeed, *Mist1*$^{LacZ/LacZ}$ pancreata exhibit hyperactive EGFR signaling, suggesting that this pathway may accelerate conversion of acinar cells to mPanINs. To determine if *Mist1*$^{LacZ/LacZ}$ acinar cells were “primed” to attain duct cell properties, we turned to a 3D *in vitro* culture system to evaluate how acinar cells from *Mist1*$^{+/+}$ and *Mist1*$^{LacZ/LacZ}$ animals responded to EGFR signaling pathways. As previously reported [28], acinar cells from control *Mist1*$^{+/+}$ mice placed in 3D collagen gels remained as acinar cells over a 5 day period (Figure 6A, a-d; 6B,C). However, when the cultures were supplemented with 10 ng/ml TGFα, a small percentage (~20%) of cells acquired duct-like properties, forming ductal cysts and expressing the duct cell product K19 (Figure 6A, e-h; 6B). Increasing TGFα to 50 ng/ml led to a maximum 45% cell conversion. In contrast, *Mist1*$^{LacZ/LacZ}$ cells were much more efficient in ductal conversion. The majority (>90%) of *Mist1*$^{LacZ/LacZ}$ acinar cells readily formed ductal cysts when placed in collagen gels containing as low as 10 ng/ml TGFα (Figure 6B,C). Indeed, even in the absence of TGFα, small (~5%) but reproducible numbers of *Mist1*$^{LacZ/LacZ}$ acinar cells spontaneously converted to ductal cysts (Figure 6B). Thus, the absence of Mist1 primes cells for ductal conversion, mimicking the accelerated mPanIN formation in *Mist1*$^{LacZ/LacZ}$/*LSL-Kras*$^{G12D/+}$ and *LSL-Kras*$^{G12D/+}$/*Mist1*$^{Cre-ER/Cre-ER}$ mice.

Discussion

Identifying the earliest events that initiate PanIN formation is critical to fully understanding the origins of pancreatic cancer. Defining PanIN development has been difficult from a clinical perspective because patients often present with advanced disease. Thus, despite some progress in disease management, there remains uncertainty about which cell types contribute to PanIN development and which intracellular pathways are critical to PanIN progression.

To examine if alterations to the acinar cell transcriptional network could affect $Kras^{G12D}$-induced early events, we evaluated the importance of Mist1, an acinar-restricted bHLH transcription factor, to mPanIN formation. Our studies demonstrated that mice lacking Mist1 were highly sensitive to $Kras^{G12D}$ expression, exhibited early acinar-ductal metaplasia ($Mist1^{Kras/+}$ model), and showed greatly accelerated mPanIN initiation and progression ($LSL\text{-}Kras^{G12D/+}$ model). Since Mist1 is not expressed in duct cells, these results reveal that altering the acinar Mist1 transcriptional network has a profound effect on the development of mPanIN lesions.

At this time, it is unclear why loss of Mist1 generates $Kras^{G12D}$ sensitivity. $Mist1^{LacZ/LacZ}$ pancreata exhibit alterations in acinar cell organization where cells acquire defects in apical-basal polarity [25], intercellular communication [32], and regulated exocytosis [33]. $Mist1^{LacZ/LacZ}$ mice also are susceptible to caerulein-induced pancreatitis [34], suggesting that dysplasia of $Mist1^{LacZ/LacZ}$ acinar cells may provide a sufficient epigenetic environment where $Kras^{G12D}$ expression efficiently initiates mPanIN development. Indeed, patients with chronic pancreatitis are more susceptible to developing PDA [35] and studies from Guerra et al. [17] have confirmed that PanIN formation is greatly enhanced in mice with chronic pancreatitis. Nonetheless, loss of Mist1 is an intrinsic event restricted to acinar cells - centroacinar cells and duct cells do not express Mist1 [20]. Thus, either dysplastic acinar cells influence the local environment to allow duct cells to develop into proliferative mPanINs or acinar cells directly participate in mPanIN formation. Although both scenarios are possible, we favor the latter for a number of reasons. First, $Mist1^{Kras/+}$ mice express $Kras^{G12D}$ exclusively from the *Mist1* locus and yet develop rare mPanIN lesions and several different pancreatic tumor types with ductal features [13]. Second, $LSL\text{-}Kras^{G12D/+}/ptf1a^{Cre/+}$ mice develop acinar metaplastic units that contain biphenotypic cells, suggesting that acinar cells contribute to mPanINs in this model [20]. Indeed, Mist1 (or β-gal) positive cells are readily identified in early mPanIN lesions in $LSL\text{-}Kras^{G12D/+}/ptf1a^{Cre/+}$ samples. Finally, lineage tracing of $LSL\text{-}Kras^{G12D/+}/Mist1^{Cre\text{-}ER/+}$ mice revealed that $Kras^{G12D}$ expressing acinar cells directly give rise to mPanIN lesions.

The transcriptional network through which Mist1 operates has yet to be defined, although several Mist1 target genes have been identified, including the gap junction gene *connexin32* [32] and the cyclin-dependent kinase inhibitor gene $p21^{CIP1/WAF1}$ [36]. Loss of both proteins is known to lead to cellular hyperplasia and it is possible that upon $Kras^{G12D}$ expression the absence of these key regulators in $Mist1^{LacZ/LacZ}$ mice accelerates acinar cells to acquire a duct-like phenotype towards mPanIN formation. The possibility also exists that loss of Mist1 during *Kras* activation is not simply a consequence of acinar metaplasia, but rather is a defined molecular pathway that is intimately associated with $Kras^{G12D}$-induced pancreas transformation. Indeed, preliminary data supports a model where the human *Mist1* locus is silenced as acinar cells undergo acinar-ductal metaplasia and PanIN formation in diseased tissues (Supplemental Figure S4) [20].

Despite a deficiency in understanding the transcriptional networks involved in tumor promotion, the signaling pathways through which activated Kras induces PDA have been well characterized, with many studies showing that the Notch and EGFR pathways are instrumental in complementing Kras signaling [21, 37]. The EGFR pathway also has been implicated in acinar-

ductal metaplasia [19, 28-30], suggesting that events controlling conversion of acinar cells to duct-like mPanINs share overlapping regulatory pathways with tumor promotion. In this current study, we showed that *Mist1*$^{LacZ/LacZ}$ acinar cells precociously activate the EGFR signaling pathway and are primed to convert to ductal cysts *in vitro*. Preliminary studies also have revealed that the Notch signaling pathway is active in *Mist1*$^{LacZ/LacZ}$ pancreata where Hes1 expressing acinar cells are readily identified (Supplemental Figure S5). This is a significant finding since induction of Notch signaling is thought to be an early event in PanIN initiation and pancreatic tumorigenesis [21, 38]. Despite precocious activation of the EGFR (pMEK1/2, pErk1/2, pStat3) and Notch (Hes1) signaling pathways in *Mist1*$^{LacZ/LacZ}$ acinar cells, activation of these pathways alone is not sufficient to generate PanIN lesions. Kras^{G12D} activity is still required. Nonetheless, acinar cells deficient in Mist1 are highly susceptible to Kras^{G12D}-induced events and show a greatly increased, accelerated rate of mPanIN formation. These results suggest that the EGFR and Notch pathways likely cooperate with a distinct Kras^{G12D} downstream pathway (*e.g.*, PI3 Kinase, RalGDS, p120-GAP) to increase the efficiency by which individual acinar cells generate PanIN lesions. Whether identical pathways converge in the human disease will have to await a more thorough analysis of PanIN progression in patients. Continued studies of the molecular pathways and transcriptional networks that operate in both normal and neoplastic pancreatic cells will be critical to delineating the individual components that lead to the generation of this deadly disease.

Supplementary Material

Refer to Web version on PubMed Central for supplementary material.

Acknowledgments

Sincere thanks go to Chris Wright for generously providing *ptf1a*$^{Cre/+}$ mice, David Tuveson for the *LSL-Kras*$^{G12D/+}$ mice and helpful discussions, Ray MacDonald for the *Elastase* promoter constructs, Pierre Chambon for the Cre-ER^{T2} cDNA, and Tetsuo Sudo for the anti-Hes1 antibody. We also thank Anna Means for assistance with the 3D acinar cell cultures, Judy Hallett and the Purdue Cancer Center TMCF for generating the mouse lines used in this study, and Michael Collingwood for assistance in generating the *Mist1*$^{Cre-ER}$ targeting construct.

Grant Support: This work was supported by grants to S.F.K. from the National Institutes of Health (DK55489, CA124586), the Phi Beta Psi Sorority Cancer Fund, and from the Lustgarten Foundation for Pancreatic Cancer. R.H.H. was supported by a NCI Specialized Program of Research Excellence grant (P50CA62924).

REFERENCES

1. Jemal A, Siegel R, Ward E, Murray T, Xu J, Smigal C, Thun MJ. Cancer statistics, 2006. CA Cancer J Clin 2006;56:106–30. [PubMed: 16514137]
2. Schneider G, Siveke JT, Eckel F, Schmid RM. Pancreatic cancer: basic and clinical aspects. Gastroenterology 2005;128:1606–25. [PubMed: 15887154]
3. Brugge WR, Lauwers GY, Sahani D, Fernandez-del Castillo C, Warshaw AL. Cystic neoplasms of the pancreas. N Engl J Med 2004;351:1218–26. [PubMed: 15371579]
4. Maitra A, Fukushima N, Takaori K, Hruban RH. Precursors to invasive pancreatic cancer. Adv Anat Pathol 2005;12:81–91. [PubMed: 15731576]
5. Maitra A, Kern SE, Hruban RH. Molecular pathogenesis of pancreatic cancer. Best Pract Res Clin Gastroenterol 2006;20:211–26. [PubMed: 16549325]
6. Hruban RH, Goggins M, Parsons J, Kern SE. Progression model for pancreatic cancer. Clin Cancer Res 2000;6:2969–72. [PubMed: 10955772]
7. Hruban RH, Adsay NV, Albores-Saavedra J, Compton C, Garrett ES, Goodman SN, Kern SE, Klimstra DS, Kloppel G, Longnecker DS, Luttges J, Offerhaus GJ. Pancreatic intraepithelial neoplasia: a new nomenclature and classification system for pancreatic duct lesions. Am J Surg Pathol 2001;25:579–86. [PubMed: 11342768]

8. Hruban RH, Adsay NV, Albores-Saavedra J, Anver MR, Biankin AV, Boivin GP, Furth EE, Furukawa T, Klein A, Klimstra DS, Kloppel G, Lauwers GY, Longnecker DS, Luttges J, Maitra A, Offerhaus GJ, Perez-Gallego L, Redston M, Tuveson DA. Pathology of genetically engineered mouse models of pancreatic exocrine cancer: consensus report and recommendations. Cancer Res 2006;66:95–106. [PubMed: 16397221]
9. Kojima K, Vickers SM, Adsay NV, Jhala NC, Kim HG, Schoeb TR, Grizzle WE, Klug CA. Inactivation of Smad4 accelerates Kras(G12D)-mediated pancreatic neoplasia. Cancer Res 2007;67:8121–30. [PubMed: 17804724]
10. Prasad NB, Biankin AV, Fukushima N, Maitra A, Dhara S, Elkahloun AG, Hruban RH, Goggins M, Leach SD. Gene expression profiles in pancreatic intraepithelial neoplasia reflect the effects of Hedgehog signaling on pancreatic ductal epithelial cells. Cancer Res 2005;65:1619–26. [PubMed: 15753353]
11. Brembeck FH, Schreiber FS, Deramaudt TB, Craig L, Rhoades B, Swain G, Grippo P, Stoffers DA, Silberg DG, Rustgi AK. The mutant K-ras oncogene causes pancreatic periductal lymphocytic infiltration and gastric mucous neck cell hyperplasia in transgenic mice. Cancer Res 2003;63:2005–9. [PubMed: 12727809]
12. Grippo PJ, Nowlin PS, Demeure MJ, Longnecker DS, Sandgren EP. Preinvasive pancreatic neoplasia of ductal phenotype induced by acinar cell targeting of mutant Kras in transgenic mice. Cancer Res 2003;63:2016–9. [PubMed: 12727811]
13. Tuveson DA, Zhu L, Gopinathan A, Willis NA, Kachatrian L, Grochow R, Pin CL, Mitin NY, Taparowsky EJ, Gimotty PA, Hruban RH, Jacks T, Konieczny SF. Mist1-KrasG12D Knock-In Mice Develop Mixed Differentiation Metastatic Exocrine Pancreatic Carcinoma and Hepatocellular Carcinoma. Cancer Res 2006;66:242–7. [PubMed: 16397237]
14. Carriere C, Seeley ES, Goetze T, Longnecker DS, Korc M. The Nestin progenitor lineage is the compartment of origin for pancreatic intraepithelial neoplasia. Proc Natl Acad Sci U S A 2007;104:4437–42. [PubMed: 17360542]
15. Jackson EL, Willis N, Mercer K, Bronson RT, Crowley D, Montoya R, Jacks T, Tuveson DA. Analysis of lung tumor initiation and progression using conditional expression of oncogenic K-ras. Genes Dev 2001;15:3243–8. [PubMed: 11751630]
16. Hingorani SR, Petricoin EF, Maitra A, Rajapakse V, King C, Jacobetz MA, Ross S, Conrads TP, Veenstra TD, Hitt BA, Kawaguchi Y, Johann D, Liotta LA, Crawford HC, Putt ME, Jacks T, Wright CV, Hruban RH, Lowy AM, Tuveson DA. Preinvasive and invasive ductal pancreatic cancer and its early detection in the mouse. Cancer Cell 2003;4:437–50. [PubMed: 14706336]
17. Guerra C, Schuhmacher AJ, Canamero M, Grippo PJ, Verdaguer L, Perez-Gallego L, Dubus P, Sandgren EP, Barbacid M. Chronic pancreatitis is essential for induction of pancreatic ductal adenocarcinoma by K-Ras oncogenes in adult mice. Cancer Cell 2007;11:291–302. [PubMed: 17349585]
18. Guerra C, Mijimolle N, Dhawahir A, Dubus P, Barradas M, Serrano M, Campuzano V, Barbacid M. Tumor induction by an endogenous K-ras oncogene is highly dependent on cellular context. Cancer Cell 2003;4:111–20. [PubMed: 12957286]
19. Strobel O, Dor Y, Alsina J, Stirman A, Lauwers G, Trainor A, Castillo CF, Warshaw AL, Thayer SP. In vivo lineage tracing defines the role of acinar-to-ductal transdifferentiation in inflammatory ductal metaplasia. Gastroenterology 2007;133:1999–2009. [PubMed: 18054571]
20. Zhu L, Shi G, Schmidt CM, Hruban RH, Konieczny SF. Acinar cells contribute to the molecular heterogeneity of pancreatic intraepithelial neoplasia. Am J Pathol 2007;171:263–73. [PubMed: 17591971]
21. Miyamoto Y, Maitra A, Ghosh B, Zechner U, Argani P, Iacobuzio-Donahue CA, Sriuranpong V, Iso T, Meszoely IM, Wolfe MS, Hruban RH, Ball DW, Schmid RM, Leach SD. Notch mediates TGF alpha-induced changes in epithelial differentiation during pancreatic tumorigenesis. Cancer Cell 2003;3:565–76. [PubMed: 12842085]
22. Pin CL, Bonvissuto AC, Konieczny SF. Mist1 expression is a common link among serous exocrine cells exhibiting regulated exocytosis. Anat Rec 2000;259:157–67. [PubMed: 10820318]
23. Johnson CL, Kowalik AS, Rajakumar N, Pin CL. Mist1 is necessary for the establishment of granule organization in serous exocrine cells of the gastrointestinal tract. Mech Dev 2004;121:261–72. [PubMed: 15003629]

24. Hingorani SR, Wang L, Multani AS, Combs C, Deramaudt TB, Hruban RH, Rustgi AK, Chang S, Tuveson DA. Trp53R172H and KrasG12D cooperate to promote chromosomal instability and widely metastatic pancreatic ductal adenocarcinoma in mice. Cancer Cell 2005;7:469–83. [PubMed: 15894267]
25. Pin CL, Rukstalis JM, Johnson C, Konieczny SF. The bHLH transcription factor Mist1 is required to maintain exocrine pancreas cell organization and acinar cell identity. J Cell Biol 2001;155:519–30. [PubMed: 11696558]
26. Zhu L, Tran T, Rukstalis JM, Sun P, Damsz B, Konieczny SF. Inhibition of Mist1 homodimer formation induces pancreatic acinar-to-ductal metaplasia. Mol Cell Biol 2004;24:2673–81. [PubMed: 15024058]
27. Feil R, Wagner J, Metzger D, Chambon P. Regulation of Cre recombinase activity by mutated estrogen receptor ligand-binding domains. Biochem Biophys Res Commun 1997;237:752–7. [PubMed: 9299439]
28. Means AL, Meszoely IM, Suzuki K, Miyamoto Y, Rustgi AK, Coffey RJ Jr, Wright CV, Stoffers DA, Leach SD. Pancreatic epithelial plasticity mediated by acinar cell transdifferentiation and generation of nestin-positive intermediates. Development. 2005
29. Sandgren EP, Luetteke NC, Palmiter RD, Brinster RL, Lee DC. Overexpression of TGF alpha in transgenic mice: induction of epithelial hyperplasia, pancreatic metaplasia, and carcinoma of the breast. Cell 1990;61:1121–35. [PubMed: 1693546]
30. Wagner M, Greten FR, Weber CK, Koschnick S, Mattfeldt T, Deppert W, Kern H, Adler G, Schmid RM. A murine tumor progression model for pancreatic cancer recapitulating the genetic alterations of the human disease. Genes Dev 2001;15:286–93. [PubMed: 11159909]
31. Siveke JT, Einwachter H, Sipos B, Lubeseder-Martellato C, Kloppel G, Schmid RM. Concomitant Pancreatic Activation of Kras(G12D) and Tgfa Results in Cystic Papillary Neoplasms Reminiscent of Human IPMN. Cancer Cell 2007;12:266–79. [PubMed: 17785207]
32. Rukstalis JM, Kowalik A, Zhu L, Lidington D, Pin CL, Konieczny SF. Exocrine specific expression of Connexin32 is dependent on the basic helix-loop-helix transcription factor Mist1. J Cell Sci 2003;116:3315–25. [PubMed: 12829745]
33. Luo X, Shin DM, Wang X, Konieczny SF, Muallem S. Aberrant localization of intracellular organelles, Ca2+ signaling, and exocytosis in Mist1 null mice. J Biol Chem 2005;280:12668–75. [PubMed: 15665001]
34. Kowalik AS, Johnson CL, Chadi SA, Weston JY, Fazio EN, Pin CL. Mice lacking the transcription factor Mist1 exhibit an altered stress response and increased sensitivity to caerulein-induced pancreatitis. Am J Physiol Gastrointest Liver Physiol 2007;292:G1123–32. [PubMed: 17170023]
35. Malka D, Hammel P, Maire F, Rufat P, Madeira I, Pessione F, Levy P, Ruszniewski P. Risk of pancreatic adenocarcinoma in chronic pancreatitis. Gut 2002;51:849–52. [PubMed: 12427788]
36. Jia D, Sun Y, Konieczny SF. Mist1 regulates pancreatic acinar cell proliferation through p21 CIP1/WAF1. Gastroenterology 2008;135:1687–97. [PubMed: 18762186]
37. Maitra A, Hruban RH. Pancreatic cancer. Annu Rev Pathol 2008;3:157–88. [PubMed: 18039136]
38. De La OJ-P, Emerson LL, Goodman JL, Froebe SC, Illum BE, Curtis AB, Murtaugh LC. Notch and Kras reprogram pancreatic acinar cells to ductal intraepithelial neoplasia. Proc Natl Acad Sci U S A 2008;105:18907–912. [PubMed: 19028876]

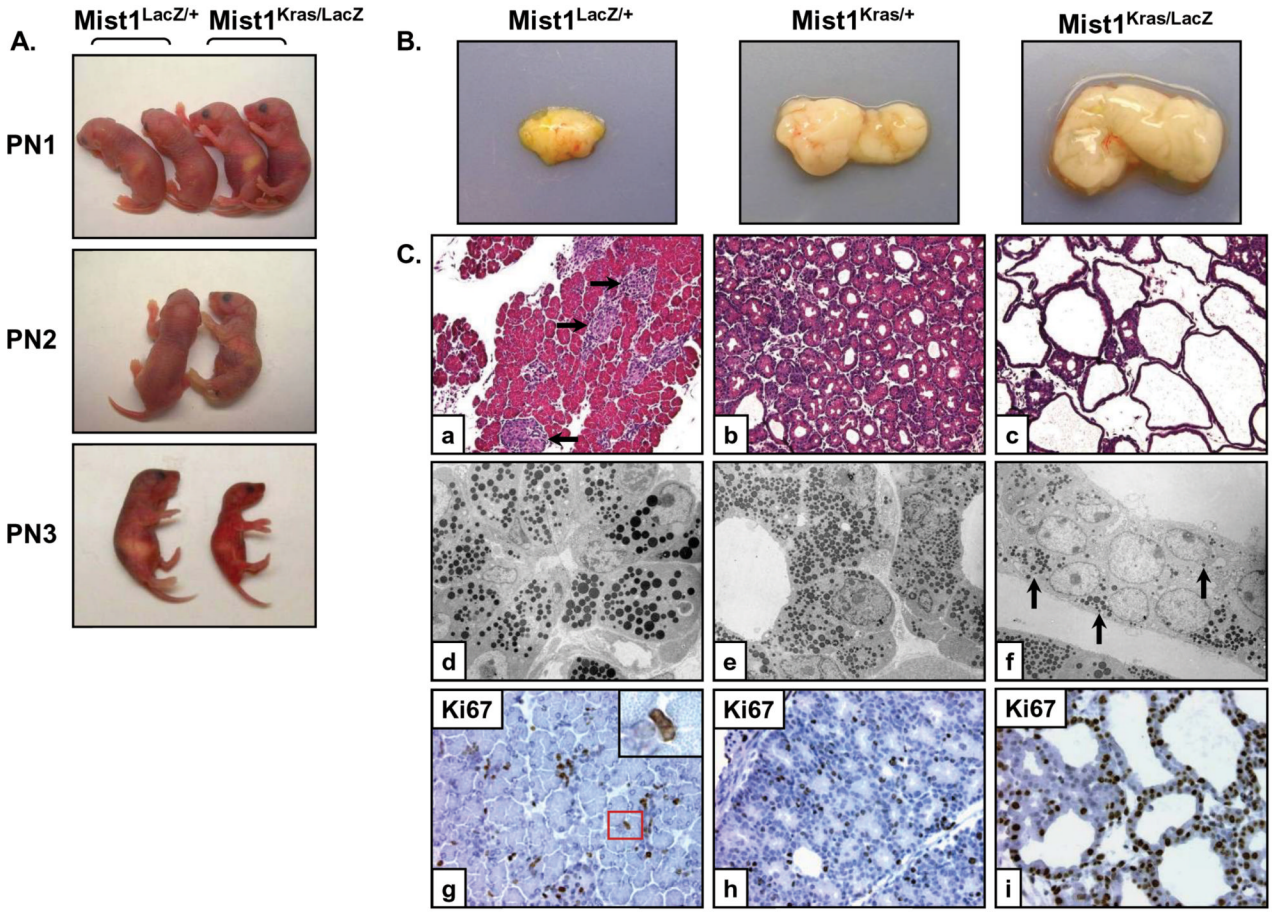

Figure 1. Mist1$^{Kras/LacZ}$ pancreas structure is grossly distorted at postnatal day 1

(A) *Mist1*$^{LacZ/+}$ and *Mist1*$^{Kras/LacZ}$ littermates in the first three days following birth. **(B)** Gross anatomy of the *Mist1*$^{LacZ/+}$, *Mist1*$^{Kras/+}$, and *Mist1*$^{Kras/LacZ}$ mouse pancreata at PN1. **(C)** (a-c) H&E sections from PN1 *Mist1*$^{LacZ/+}$, *Mist1*$^{Kras/+}$, and *Mist1*$^{Kras/LacZ}$ pancreata (x200). Arrows in (a) indicate islets. (d-f) Transmission electron microscopy of PN1 pancreas samples. The tubular networks that form in the *Mist1*$^{Kras/LacZ}$ samples exhibit greatly reduced zymogen granules (arrows) and crowding of nuclei (x1,100). (g-i) Immunohistochemistry labeling with Ki67 reveals a higher proliferation index in the *Mist1*$^{Kras/LacZ}$ mice at PN1 (x400). Note that most Ki67 positive cells in (g) are interstitial cells that lie between acini (inset).

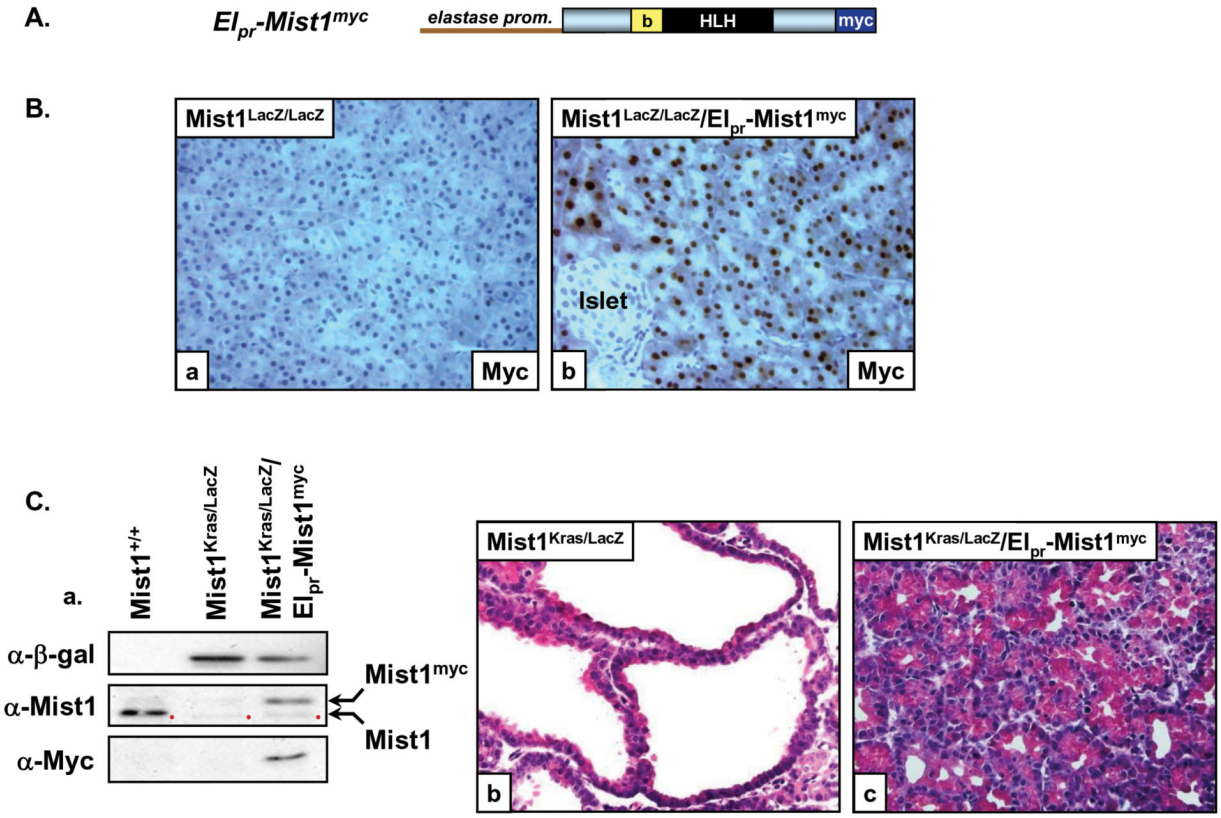

Figure 2. Ectopic expression of Mist1^{myc} rescues the Mist1$^{Kras/LacZ}$ phenotype

(A) *El$_{pr}$-Mist1^{myc}* transgene. b, basic domain; HLH, helix-loop-helix domain; myc, epitope tag. **(B)** Immunohistochemistry using anti-myc on *Mist1$^{LacZ/LacZ}$* and *Mist1$^{LacZ/LacZ}$/El$_{pr}$-Mist1^{myc}* pancreas sections showing acinar-specific expression of the *El$_{pr}$-Mist1^{myc}* transgene (x400). **(C)** (a) Immunoblot analysis of extracts from *Mist1$^{+/+}$*, *Mist1$^{Kras/LacZ}$*, and *Mist1$^{Kras/LacZ}$/El$_{pr}$-Mist1^{myc}* pancreata. β-gal protein is expressed from the *Mist1* locus in the *Mist1$^{Kras/LacZ}$* and *Mist1$^{Kras/LacZ}$/El$_{pr}$-Mist1^{myc}* pancreata. The Mist1^{myc} protein is detected only in the *Mist1$^{Kras/LacZ}$/El$_{pr}$-Mist1^{myc}* samples. Red dots - nonspecific bands from the Mist1 antibody. (b, c) *El$_{pr}$-Mist1^{myc}* expression rescues the severe *Mist1$^{Kras/LacZ}$* phenotype (x400).

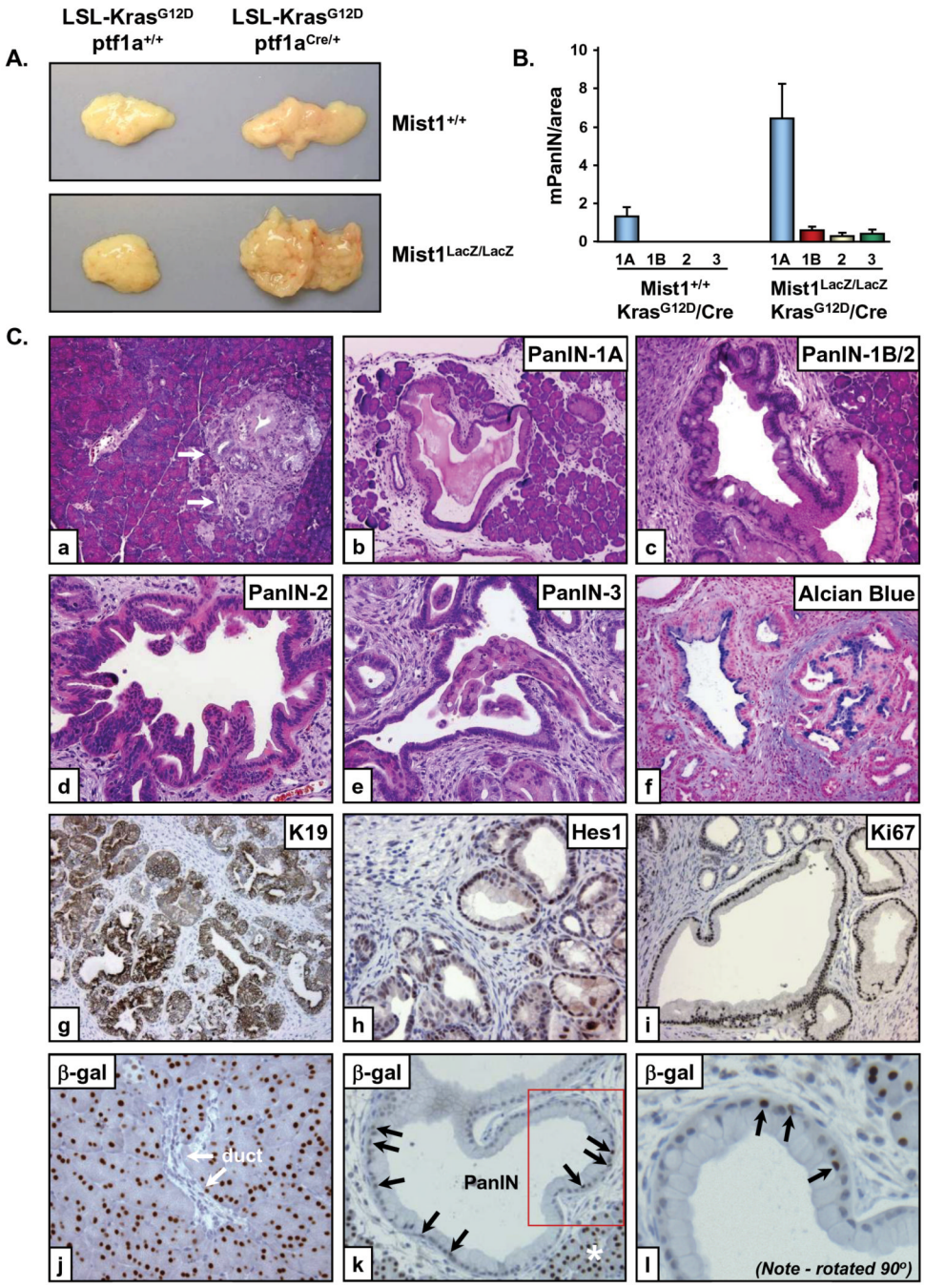

Figure 3. Mist1$^{LacZ/LacZ}$/LSL-Kras$^{G12D/+}$/ptf1a$^{Cre/+}$ pancreata display accelerated histological progression of mPanIN lesions at early stages

(A) Gross anatomy of the *Mist1$^{LacZ/LacZ}$/LSL-Kras$^{G12D/+}$/ptf1a$^{Cre/+}$* versus *Mist1$^{+/+}$/LSL-Kras$^{G12D/+}$/ptf1a$^{Cre/+}$* pancreata at 6 weeks. **(B)** Quantitative analysis of mPanIN lesions in 6 week *Mist1$^{+/+}$/LSL-Kras$^{G12D/+}$/ptf1a$^{Cre/+}$* and *Mist1$^{LacZ/LacZ}$/LSL-Kras$^{G12D/+}$/ptf1a$^{Cre/+}$* samples (n=4). Note that high-grade mPanIN-1B, mPanIN-2 and mPanIN-3 are never observed in the *Mist1$^{+/+}$/LSL-Kras$^{G12D/+}$/ptf1a$^{Cre/+}$* mice at this age. **(C)** High-grade mPanIN lesions rapidly develop in *Mist1$^{LacZ/LacZ}$/LSL-Kras$^{G12D/+}$/ptf1a$^{Cre/+}$* pancreata. (a) 6-week *Mist1$^{+/+}$/LSL-Kras$^{G12D/+}$/ptf1a$^{Cre/+}$* pancreas showing a rare focus of mPanIN-1A (arrows) (x100). (b-l) Representative images from *Mist1$^{LacZ/LacZ}$/LSL-Kras$^{G12D/+}$/ptf1a$^{Cre/+}$* samples (6 week).

mPanIN-1A lesions are broadly distributed (b, x100) with early appearance of higher grade mPanIN-1B (c, x200), mPanIN-2 (d, x200) and mPanIN-3 (e, x200) lesions. (f) Alcian blue staining reveals abundant mucin content in the mPanIN lesions. K19 (g), Hes1 (h) and Ki67 (i) are highly expressed in the *Mist1*$^{LacZ/LacZ}$/*LSL-Kras*$^{G12D/+}$/*ptf1a*$^{Cre/+}$ mPanIN lesions. (j) β-gal immunohistochemistry on *Mist1*$^{LacZ/LacZ}$/*LSL-Kras*$^{G12D/+}$ control samples revealing nuclear β-gal only in acinar cells. (k,l) β-gal positive nuclei are found within large PanINs from *Mist1*$^{LacZ/LacZ}$/*LSL-Kras*$^{G12D/+}$/*ptf1a*$^{Cre/+}$ samples (arrows). Boxed area in (k) is shown at higher magnification in (l). Asterisk in (k) denotes normal acinar tissue.

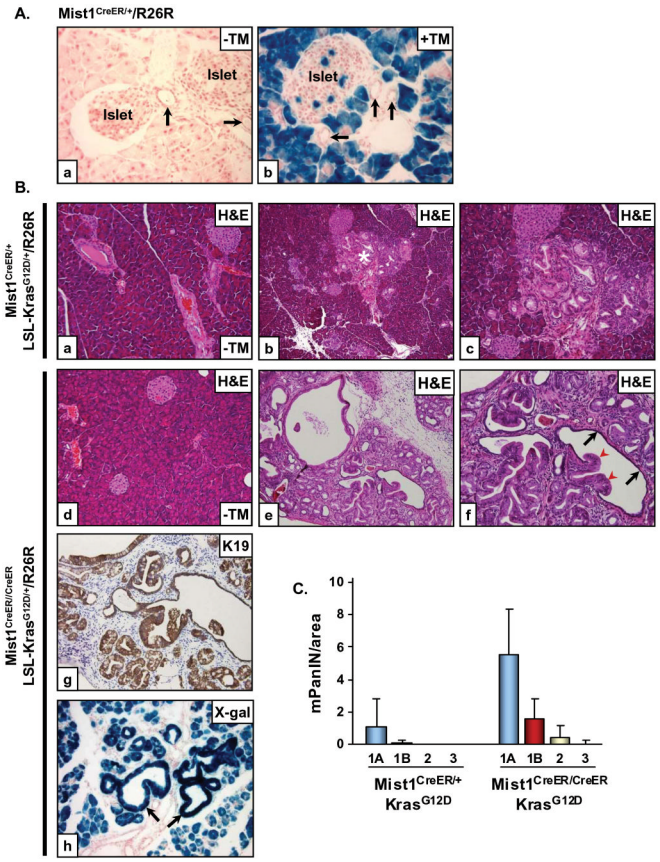

Figure 4. LSL-Kras$^{G12D/+}$/Mist1$^{Cre-ER/+}$ mice reveal that acinar cells generate mPanIN lesions

(A) *Mist1$^{Cre-ER/+}$/R26R* adult mice were given a single dose of corn oil (a) or tamoxifen (TM) (b) for three consecutive days and then pancreata were harvested and processed for β-gal detection 2 weeks later. Acinar cells and rare islet cells are β-gal+ whereas all duct cells (arrows) remain β-gal negative (x400). **(B)** Adult 6 week *LSL-Kras$^{G12D/+}$/Mist1$^{Cre-ER/+}$/R26R* (a-c) and *LSL-Kras$^{G12D/+}$/Mist1$^{Cre-ER/Cre-ER}$/R26R* (d-f) mice were administered corn oil (a,d, x200) or tamoxifen (b,c, x100; e,f, x200) and pancreata were analyzed at 3 months of age. *LSL-Kras$^{G12D/+}$/Mist1$^{Cre-ER/Cre-ER}$/R26R* pancreata develop advanced mPanINs which express high levels of K19 (g, x200). (h) β-gal+ mPanINs (arrows) confirm the acinar cell origin of these lesions (x200). Arrows in (f) indicate mPanIN extensions (red) and fusion with normal ductal epithelial (black). **(C)** Quantitative analysis of mPanIN lesions in 6 week *LSL-Kras$^{G12D/+}$/Mist1$^{Cre-ER/+}$* and *LSL-Kras$^{G12D/+}$/Mist1$^{Cre-ER/Cre-ER}$* mice treated with tamoxifen (n=4). Note the large increase in all mPanIN grades in the *LSL-Kras$^{G12D/+}$/Mist1$^{Cre-ER/Cre-ER}$* (*Mist1^{KO}*) mice.

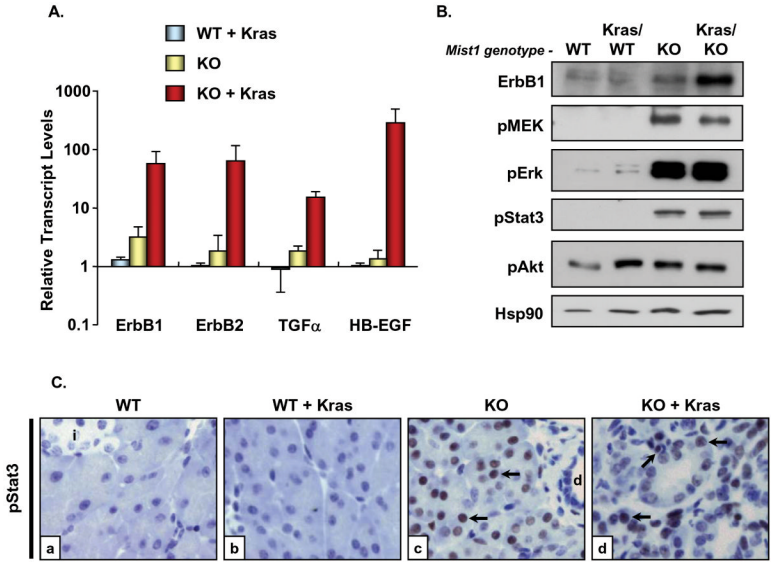

Figure 5. Mist1$^{LacZ/LacZ}$ and Mist1$^{LacZ/LacZ}$/LSL-Kras$^{G12D/+}$/ptf1a$^{Cre/+}$ pancreata exhibit elevated levels of EGFR signaling components and activation of downstream signaling pathways

(A) Quantitative RT-PCR to detect *ErbB1*, *ErbB2*, *TGFα*, and *HB-EGF* transcript levels from the indicated pancreata samples. All values were normalized to *Mist1*$^{+/+}$ (WT) samples which were set to 1.0. **(B)** Immunoblots for a number of EGFR signaling components. In all cases, *Mist1*$^{LacZ/LacZ}$ (KO) and *Mist1*$^{LacZ/LacZ}$/*LSL-Kras*$^{G12D/+}$/*ptf1a*$^{Cre/+}$ (KO + Kras) samples exhibited activation of the downstream pathways, with the exception of pAKT, which did not significantly change with different genotypes. Hsp90 was used as a loading control. **(C)** Immunohistochemistry with anti-pStat3 reveals that acinar cells in the *Mist1*^{KO} background are pStat3 positive (arrows). Duct (d) and islet (i) cells remain pStat3 negative, as do acinar cells in a *Mist1*^{WT} background (x800).

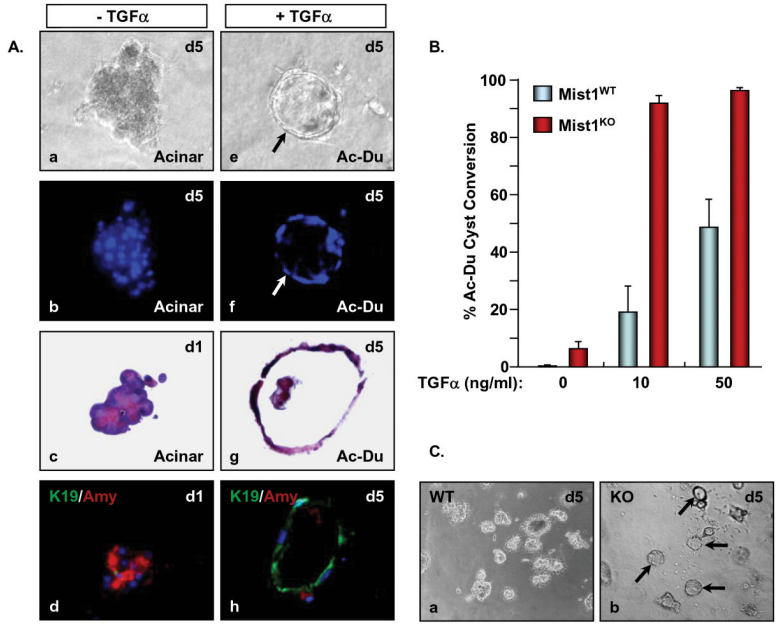

Figure 6. Mist1$^{LacZ/LacZ}$ acinar cells rapidly convert to ductal cysts in 3D collagen cultures

(A) Acinar cells were isolated from *Mist1*$^{+/+}$ pancreata and cultured in collagen gels in the presence or absence of TGFα. Cells in control medium without TGFα (a-d, x800) maintain a normal amylase positive acinar cell phenotype while cells supplied TGFα (e-h, x800) convert to K19 positive ductal cysts (arrow) (b,f - Dapi fluorescence; c.g - H&E sections; d,h - K19 and amylase co-immunofluorescence). **(B)** *Mist1*$^{LacZ/LacZ}$ acinar cells exhibit a propensity to convert to ductal cysts, even in the absence of TGFα. **(C)** Nearly all *Mist1*$^{LacZ/LacZ}$ acinar cells convert to ductal cysts after 5 days in 10 ng/ml TGFα whereas *Mist1*$^{+/+}$ cells remain as acinar cell clusters (x200).